Research Article

NMR IN BIOMEDICINE

Received: 17 December 2008, Revised: 24 August 2009, Accepted: 2 September 2009, Published online in Wiley InterScience: 1 December 2009

(www.interscience.wiley.com) DOI:10.1002/nbm.1462

Reliability and precision of pseudo-continuous arterial spin labeling perfusion MRI on 3.0 T and comparison with ^{15}O-water PET in elderly subjects at risk for Alzheimer's disease

Guofan Xu[a,b]*, Howard A. Rowley[c], Gaohong Wu[f], David C. Alsop[e], Ajit Shankaranarayanan[f], Maritza Dowling[g], Bradley T. Christian[d], Terrence R. Oakes[d] and Sterling C. Johnson[a,b]

Arterial spin labeling (ASL) offers MRI measurement of cerebral blood flow (CBF) *in vivo*, and may offer clinical diagnostic utility in populations such as those with early Alzheimer's disease (AD). In the current study, we investigated the reliability and precision of a pseudo-continuous ASL (pcASL) sequence that was performed two or three times within one hour on eight young normal control subjects, and 14 elderly subjects including 11 with normal cognition, one with AD and two with Mild Cognitive Impairment (MCI). Six of these elderly subjects including one AD, two MCIs and three controls also received ^{15}O-water positron emission tomography (PET) scans 2 h before their pcASL MR scan. The instrumental reliability of pcASL was evaluated with the intraclass correlation coefficient (ICC). The ICCs were greater than 0.90 in pcASL global perfusion measurements for both the young and the elderly groups. The cross-modality perfusion imaging comparison yielded very good global and regional agreement in global gray matter and the posterior cingulate cortex. Significant negative correlation was found between age and the gray/white matter perfusion ratio ($r = -0.62$, $p < 0.002$). The AD and MCI patients showed the lowest gray/white matter perfusion ratio among all the subjects. The data suggest that pcASL provides a reliable whole brain CBF measurement in young and elderly adults whose results converge with those obtained with the traditional ^{15}O-water PET perfusion imaging method. pcASL perfusion MRI offers an alternative method for non-invasive *in vivo* examination of early pathophysiological changes in AD. Copyright © 2009 John Wiley & Sons, Ltd.

Supporting information may be found in the online version of this article.

Keywords: cerebral blood flow (CBF); perfusion; arterial spin labeling (ASL); Alzheimer's disease (AD); magnetic resonance imaging (MRI); positron emission tomography (PET)

INTRODUCTION

Different neuroimaging techniques, including single-photon emission computed tomography (SPECT), positron emission tomography (PET), and magnetic resonance imaging (MRI) techniques, have all shown the capability of detecting early brain perfusion deficits related to Alzheimer's disease (AD) (1–4). MRI-based arterial spin labeling (ASL) magnetically labels the protons in blood for use as a tracer to measure cerebral blood flow (CBF), without injection of exogenous contrast agent (5). Since ASL is free of radiation and non-invasive, it may be particularly useful in situations that call for repeat examination,

* *Correspondence to: G. Xu, GRECC, Madison VA Hospital, Madison, WI, USA.*

a *G. Xu, S. C. Johnson*
GRECC, Madison VA Hospital, Madison, WI, USA

b *G. Xu, S. C. Johnson*
Department of Medicine, University of Wisconsin – Madison, WI, USA

c *H. A. Rowley*
Department of Radiology, University of Wisconsin – Madison, WI, USA

d *B. T. Christian, T. R. Oakes*
Department of Psychiatry and Medical Physics, University of Wisconsin – Madison, WI, USA

e *D. C. Alsop*
Department of Radiology, Beth Israel Deaconess Medical Center and Harvard Medical School, Cambridge, MA, USA

f *G. Wu, A. Shankaranarayanan*
GE healthcare, Milwaukee, WI, USA

g *M. Dowling*
Department of Biostatistics and Medical Informatics, University of Wisconsin – Madison, WI, USA

Contract/grant sponsor: Merit Review Grant from the Department of Veterans Affairs.
Contract/grant sponsor: NIH; contract/grant numbers: AG21155, AG20013, AG27161, EB007021-03.

Abbreviations used: *AD, Alzheimer's disease; ASL, arterial spin labeling; CBF, cerebral blood flow; MRI, magnetic resonance imaging; PET, positron emission tomography.*

NMR IN BIOMEDICINE

such as in monitoring longitudinal changes associated with disease progression or treatment response in clinical trials.

CBF is tightly coupled to focal neural function (6) and has been shown relatively stable over time (7). Using ASL-based MRI methods, regional CBF perfusion deficits have previously been reported in patients with Alzheimer's disease (AD) and patients with mild cognitive impairment (MCI), who are at greater risk for developing AD (4,8,9). These findings suggest the brain perfusion measurement as a potential neuroimaging tool for characterizing functional brain changes that occur early in the course of AD.

In order to apply the ASL technique in large scale longitudinal AD studies, drug treatment trials and potentially in the routine radiologic evaluation of AD, the reliability and precision of the ASL technique need to be carefully evaluated. The precision of ASL in comparison to the gold standard ^{15}O-water PET perfusion method has previously been reported in young control subjects. CBF in cortical regions had similar values in MR-ASL and PET methods (10,11). Meanwhile, the white matter (WM) perfusion values obtained with ASL images are often underestimated and its applicability is limited due to the poor signal-to-noise ratio (SNR) and heterogeneous arterial transit time in WM (12).

Several studies have evaluated the ASL test-retest reliability with both pulse or continuous labeling techniques (7,13–15). However, these previous ASL studies were done either with young controls subjects or on 1.5 Tesla scanners that provide less optimal ASL SNR. The reliability and reproducibility of ASL measurements are potentially restricted by the low SNR in subtracted images (13). Given the finding that the perfusion weighted signals in elderly is less than those of young subjects (16), a reliable measurement of perfusion among the elderly population could be challenging with the usually limited allowable scan time.

Recent technical advancement in pseudo-continuous ASL (pcASL) significantly increased the flow labeling efficacy within a single coil setting (17,18). Also, ASL at 3.0 T is expected to improve the image quality and reduce transit-related effects on perfusion images by taking advantage of the increased T1 relaxation time and SNR at high field strengths (19). When combined with background static signal suppression, the new optimized pcASL sequence dramatically increased the perfusion sensitivity (17,18) and could possibly lead to a more reliable ASL perfusion measure among aging population.

Here we used this latest ASL advancement to generate quantitative CBF images in both young controls and elderly with varying levels of AD risk or disease severity. The enhanced ASL CBF method allowed us to study the relationship between age and CBF with increased SNR. With a repeated experimental design, the within-subject reproducibility and between-subject reliability were evaluated in both young and elderly subjects. The cross-modality agreement of regional CBF measurement with this optimized ASL technique and ^{15}O-water PET scan was evaluated among six elderly subjects.

METHOD

Participants

A total of 22 subjects were recruited in this study including eight young controls (four men and four women, age range: 24–40 years, mean 31) and 14 older adults (six men and eight women, age range: 50–73 years, mean 61). In order to match the prevalence of AD in the older population, one AD and two MCI patients were included as positive controls whose diagnoses were based on consensus conference case reviews. The rest of the older individuals were selected from a carefully characterized cohort known as The Wisconsin Registry for AD Prevention (WRAP), many of whom have a parent with AD and are considered at high risk to develop AD (20). The study was approved by the Institutional Review Board at the University of Wisconsin. All participants provided informed consent prior to participation. The consent process included an initial screening for MRI and PET compatibility and discussion of major safety exclusion criteria. Study exclusion criteria included contraindications to MRI and PET; less than ten years of education; pregnancy; major head trauma, psychiatric disease such as schizophrenia and substance dependence, or abnormal structural MRI and neuropsychological testing as part of study participation. Excluded medications include psychoactive medications, neuroleptics, short or long acting nitrates, and warfarin or other drugs that may affect CBF (such as caffeine within 3 h and nicotine within 1 h of the imaging exam).

Imaging Protocol

Magnetic resonance imaging

All MR studies were conducted on a 3.0 T clinical short bore MR scanner (GE Medical System, Milwaukee, WI) with the manufacturer's receive-only eight-channel array head coil and the body transmit coil. T2-weighted spin-echo and fluid attenuated inversion recovery (FLAIR) sequences were acquired and used only for radiological evaluation to exclude anatomical abnormalities. An axial slice-selective inversion recovery fast spin echo sequence (IR-FSE: TE/TR 26/4000 ms, $0.9375 \times 0.9375 \times 4$ mm,) was repeatedly performed with variable TI (100–3500 ms in ten increments) on a single oblique axial slice that covers the corpus callosum and sagittal sinus. It is intended to obtain WM and blood T1 relaxation time for the ASL CBF quantification.

For each young subject, the ASL test–retest examinations were repeated three times within 1 h. The subjects were moved out of the scanner for a 20–30 min break between the 2nd and 3rd ASL scans. For elderly subjects, two ASL scans were run in the same scanning session with a 30–40 min interval in between. The anatomical scans as well as T1 measurement were performed between the two ASL perfusion scans. The landmarks were reset between ASL scans and auto prescans were performed to adjust the receiver gain automatically. Separate high order shimming protocol was performed before each ASL scan for the adjustment of potential shifts in patient brain location.

CBF imaging with 3D pcASL

The cerebral blood flow images were acquired with 3D pcASL sequence that uses a pseudo-continuous labeling technique (17) and a fast spin echo acquisition with an interleaved stack of spiral (outward direction) readout and a centric ordering in the slice encoding direction. Each spiral arm included 512 sampling points in k-space and a total of 8 interleaves (arms) were acquired separately with a repetition time (TR) of 6 sec and an echo train length of 40. The echo spacing was 7 ms and the effective echo time was 21 ms. The field of view (FOV) was $24 \times 24 \times 16$ cm. Reconstruction was performed using a Fourier transform algorithm after the k-space data were regridded into $64 \times 64 \times 40$ matrix. As shown in Figure 1A, the sequence employed repeated selective saturation of the slab at 4.3 sec

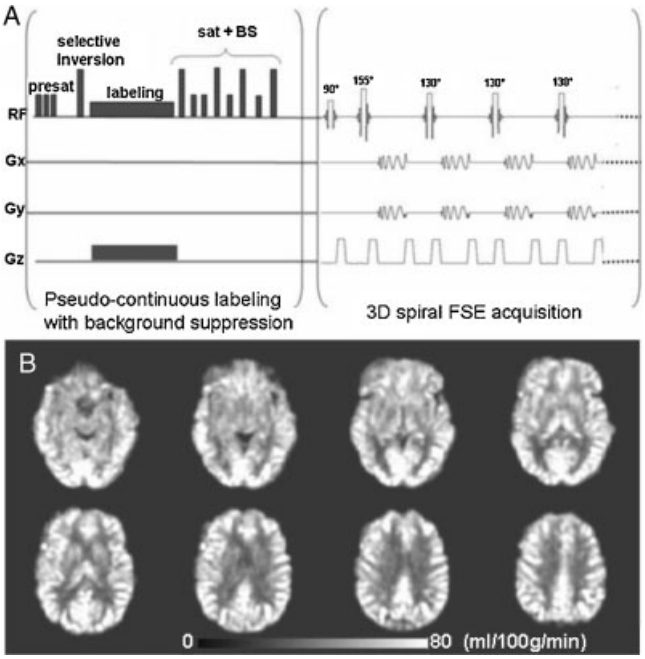

Figure 1. (A) 3D pseudo-continuous arterial spin labeling (pcASL) pulse sequence paradigm. Presat: pre-saturation pulse; sat: saturation pulse; BS: background suppression. (B) A set of cerebral blood flow (CBF) images from one 57-year old control subject with pcASL scan. The ASL perfusion image voxel size is $3.75 \times 3.75 \times 4\ mm^3$. FSE acquisition: Fast Spin Echo acquisition.

before image (pre-saturation), a slab selective inversion at 3 sec before imaging, pseudo-continuous labeling from 3 sec to 1.5 sec before imaging, and saturation plus nonselective inversion before imaging. The after-labeling saturation and inversion were used to reduce the background signal from the static spins to less than 2% of normal (21), which greatly reduced motion artifacts and the dynamic range requirements for whole brain 3D imaging.

Pseudo-continuous labeling was performed with a published method for multi-slice spin labeling with a single coil that virtually eliminates off-resonance errors (17). It utilizes a train of discrete RF pulses to mimic continuous tagging by flow-driven adiabatic inversion that does not require continuous RF transmit (17,18). A labeling RF amplitude of 0.24 mG and a gradient amplitude of 1.6 mT/m were employed. Label and control were alternately applied every 6 sec (TR). A pair of the label and control whole-brain image volumes required a total of 96 sec. The label and control images were subtracted to produce an ASL difference image. One ASL scan included an average of three ASL difference images that required a total of 288 sec scan time. Immediately after each ASL scan, a reference scan was performed with identical imaging acquisition parameters except for a saturation pulse at 2.0 sec and no ASL labeling. This fluid suppressed proton density (PD) image was used for calculating the sensitivity map during ASL flow quantification as well as for imaging registration.

MRI CBF calculation

A T1 map was first derived by fitting the multi-TI inversion-recovery fast spin echo (IR-FSE) image series using the standard model:

$$S_{(t)} = M_0\left(1 - 2A\exp\left(\frac{-t}{T1}\right)\right) \quad (1)$$

where A is the 180° pulse inversion efficacy. Regions of interest (ROI) were manually drawn on the IR-FSE images including the corpus callosum white matter ROI and sagittal sinus ROI. The T1 values of blood and WM were obtained by averaging the fitted T1 values among the voxels with a goodness of fit ($p < 0.001$) within these two ROIs.

For quantification of flow, it was necessary to calibrate the sensitivity of the image to water at each voxel (22–24). Using a maximum neighborhood algorithm to avoid regions with partial volume of suppressed fluid, a sensitivity map *C* was created with the equation:

$$C = PD/\left(C_{WM}\left(1 - \exp\left(\frac{-T_{sat}}{T1_{WM}}\right)\right)\right) \quad (2)$$

where *PD* is the flow saturated proton density image intensity; C_{MW} is the assumed white matter tissue water concentration of 0.8 gm/ml (25), T_{sat} is the saturation time of 2 sec in the flow attenuated PD image, and $T1_{WM}$ is the WM T1 value derived from fitting the IR-FSE images. This calibration produced a sensitivity map, *C*, equal to the fully relaxed MRI signal intensity produced by one gm of water per ml of brain (22,26). With this co-registered sensitivity map *C*, we calculated cerebral blood flow (CBF) using the equation:

$$CBF = \frac{\rho_b(S_c - S_l)}{2\alpha C\ \omega_a T1_a \exp\left(-\frac{w}{T1_a}\right)\left(1 - \exp\left(-\frac{tl}{T1_a}\right)\right)} \quad (3)$$

where ρ_b is the density of brain tissue, 1.05 g/ml (25), α is the labeling efficiency, assumed to be 85% (27,28) for labeling multiplied by 75% for background suppression (29), *w* is the post-labeling delay (23), 1.5s, *tl* is the labeling duration, 1.5 sec, $T1_a$ is the T1 of arterial blood, obtained by fitting the T1 measurement, ω_a is the density of water in blood, 0.85 g/ml (25), and S_l and S_c are the signal intensities in the labeled and control images, respectively.

PET ^{15}O-water scan

The PET studies were performed in 3D mode on a GE Advance PET scanner (GE Medical Systems, Milwaukee, WI). This is a scanner with an axial field of view (FOV) of 14.6 cm and a reconstructed in-plane resolution of 7–8 mm. Before positioning the patients in the scanner, catheters were placed in the left antecubital veins for tracer infusion. The head of each patient was restrained in a head holder to minimize movement artifacts. Before the ^{15}O-water administration, a 10 min transmission scan was acquired for photon attenuation correction. For each subject, 400–600 MBq ^{15}O-water was injected as a rapid bolus (<5 sec). A series of fourteen dynamic frames were acquired for a total of 2 min following injection. The data were reconstructed using filtered back projection (128×128 matrix, 35 slices, $2 \times 2 \times 4.25$ mm voxel size) with standard corrections for random events, attenuation and scatter. Each subject had three repeated ^{15}O-water PET CBF scans with an interval of at least 10 min between injections to allow for the decay of radioactivity.

Image Analysis

For each individual ^{15}O-water PET scan, the CBF image was obtained by integrating the frames over 60 seconds upon the arrival of the bolus of ^{15}O-water tracer to the brain (30). The integrated image was then normalized to a grand mean of the whole brain flow to obtain the relative CBF image. Within each

NMR IN BIOMEDICINE

Table 1. Reliabilty of cerebral blood flow measured by pcASL-MRI

ICC values	Gray matter	White matter	PCC	Temporal lobe	Frontal lobe	Parietal lobe	Frontal-temporal	Occipital lobe
Elderly subjects	0.93	0.82	0.96	0.89	0.93	0.96	0.95	0.98
95% CI	0.731–0.981	0.271–0.955	0.833–0.989	0.625–0.972	0.752–0.983	0.834–0.989	0.828–0.988	0.921–0.995
Young subjects	0.931	0.957	0.801	0.919	0.943	0.936	0.933	0.888
95% CI	0.789–0.984	0.856 –0.991	0.488–0.952	0.757–0.982	0.824–0.987	0.803–0.986	0.797–0.985	0.678–0.974

pcASL-MRI repeated three scans for young controls and twice for elderly subjects.
CI, confidence Interval; ICC, Intraclass correlation coefficient.

subject, the three perfusion images were co-registered to the average image with rigid body transformations. All co-registered perfusion images were subsequently warped to the Montreal Neurological Institute template (MNI) with Statistical Parametric Mapping (SPM5) software (www.fil.ion.ucl.ac.uk/spm5) using the non-linear normalization function with preserving concentration option.

Each subject's PD image was used as reference to estimate the normalization transformation matrix with which the ASL CBF maps were subsequently spatially nonlinear normalized to a MNI template with SPM5. All pcASL and PET CBF images were smoothed with a 8 mm full width half maximum Gaussian kernel filter after normalization. A predefined set of standard regions of interest (ROIs) including global gray matter (GM), frontal, temporal, parietal, temporal parietal, occipital lobes and posterior cingulate cortex (PCC) (WFU PickAtlas Tool, Wake Forest Univ. http://fmri.wfubmc.edu/cms/software) were used as templates for ROI analysis. In order to avoid GM-WM contamination, WM ROIs were manually selected on each subject's perfusion weighted images using a previously published approach (12). The mean and standard deviation of CBF across all subjects were obtained in these above ROIs.

For both the MRI and PET perfusion signal to noise ratio (SNR) calculation, the published method was applied (12). In brief, the ROIs of background thermal noise, GM and WM were manually selected on each subject's perfusion weighted images using the same approach published previously (12). The perfusion SNR was calculated by dividing the perfusion signal amplitude by the thermal noise variance in the perfusion weighted image. Both the PET and ASL perfusion SNRs were scaled by the square root of 3 to reflect the effect of averaging.

The test–retest reliability of pcASL scans was evaluated with the classic intraclass correlation coefficient (ICC) (31) defined as:

$$ICC = \frac{MS_{BS} - MS_{WS}}{MS_{BS} + (k-1)MS_{WS}} \quad (4)$$

where MS_{BS} is the variance between subjects and MS_{WS} is the variance within subjects, and k is number of measurements.

Bland-Altman plots were generated to display the spread of data and to evaluate the measurement agreement between ^{15}O-water PET and MR pcASL normalized relative cerebral blood flow (rCBF) images (32). Linear regression models were used to estimate the association between rCBF values measured by the two methods as well as the association between age and CBF.

RESULTS

The 3D pcASL pulse sequence paradigm is plotted in Figure 1A. The 8-channel coil has a heterogeneous sensitivity profile and it caused signal non-uniformity in the raw perfusion weighted images. Such signal non-uniformity was corrected during the CBF quantification process by dividing the subtraction image with the water sensitivity map derived from the PD image, which contained the same coil sensitivity profile. A representative ASL CBF images from a 57-year-old elderly subject is shown in Figure 1B. For each subject, the ASL quantitative CBF images were used for reliability assessments.

The test–retest reliability exam of the pc-ASL CBF images was evaluated by ICC. All the ROIs' ICC values are summarized in Table 1 and show that perfusion measurements achieve high reliability in both young and older subjects. The highest ICC values are 0.957 from the white matter ROI in young controls and 0.98 in occipital lobes in elderly subjects. The lowest ICC values are 0.80 from PCC in young controls and 0.89 in temporal lobes from elderly subjects. The measurement reliability is not significantly different between the young controls and the elderly subjects over all ROIs ($p = 0.28$, paired t-test of ICC values). As shown in Table 2, the regional ASL CBF values were listed in units of ml/100g/min. The mean and standard deviation (SD) are calculated separately from all the scans within each age group (young and elderly subjects). An overall trend of slight CBF decrease with aging was found across all the ROIs. However, none of these ROI CBF values showed statistically significant differences between young and elderly subjects. The perfusion

Table 2. The global gray matter and white matter ROI mean and standard deviation of CBF values

ASL CBF ROI value (ml/100g/min)	Young subjects		Elderly subjects	
	Mean	STD	Mean	STD
GM (global)	48.02	7.63	43.18	12.03
WM (global)	20.16	3.93	21.50	4.61
PCC	60.37	6.47	56.80	12.10
Temporal lobe	41.73	8.78	35.92	9.68
Frontal lobe	43.11	9.29	34.57	9.86
Parietal lobe	45.69	10.01	36.72	14.59
Frontal-Temporal Lobe	42.31	8.71	35.22	12.50
Occipital lobe	42.80	8.30	39.85	15.03

Table 3. The perfusion signal to noise ratio (SNR) comparison

	ASL (young subjects)		ASL (elderly subjects)		PET (elderly subjects)	
Perfusion SNR	Mean	STD	Mean	STD	Mean	STD
GM ROI	13.83	2.81	8.86	2.07	6.40	1.20
WM ROI	0.95	0.33	0.68	0.09	0.97	0.07

The perfusion SNR is the perfusion signal amplitude compared to the image background noise, scaled by square root of 3 to reflect the effect of average.

SNR from both young and elderly subjects acquired with pcASL and ^{15}O-water PET methods were listed on Table 3.

There were six elderly subjects (one AD, two MCI and three elderly controls) who had both ^{15}O-water PET and pcASL MR scans. One representative elderly subject's MRI and PET perfusion images are shown in Fig. 2A. The GM, WM and PCC ROIs are displayed in Fig. 2B. As shown in the Bland–Altman plot (Fig. 2C) the two perfusion imaging modalities showed overall good agreement on the normalized rCBF values across GM, WM & PCC ROIs. The averaged data points are within ± 2 SD from the mean difference (i.e. a 95% CI). However, an outliner seemed to occur on GM and PCC rCBF values (Supplementary Fig. 1). The correlation coefficients (CC) of regional perfusion rates are 0.742 in global GM ($p < 0.091$), 0.789 in PCC ($p < 0.057$) and 0.772 in WM ($p < 0.072$). These correlations are plotted in Fig. 2D.

The relationship between cerebral blood flow and age is explored in Figure 3, where the pcASL CBF in global GM, WM and GM/WM ratio values are plotted against the subject's age. A strong negative correlation is found between GM/WM CBF ratio and age (CC $= -0.62$, $p < 0.002$). However, a Student's *t*-test showed no significant difference between the current young and elderly subjects both in global GM and in WM CBF. While a weak negative

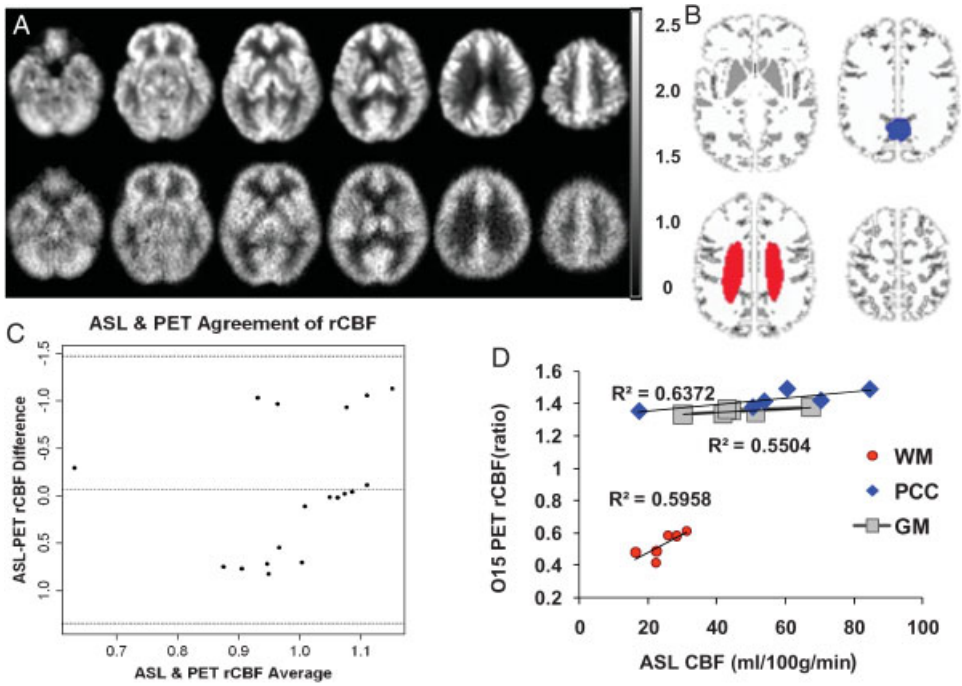

Figure 2. (A) Grand mean normalized regional CBF (rCBF) images from one 60-year old control with normal cognition using pcASL-MRI (upper row) and ^{15}O-water PET (bottom row) method. The rCBF images are in the same ratio scale; (B) Mask template shows GM in gray and PCC in blue (WFU PickAtlas Tool). WM ROI is manually drawn for each subject and shown in red. (C) Bland–Altman plots show the agreement on rCBF from GM, WM and PCC measured by pcASL-MRI and ^{15}O-water PET methods. D. In the scatter plot, significant correlations were shown in the CBF perfusion values from both the GM, WM and PCC ROIs.

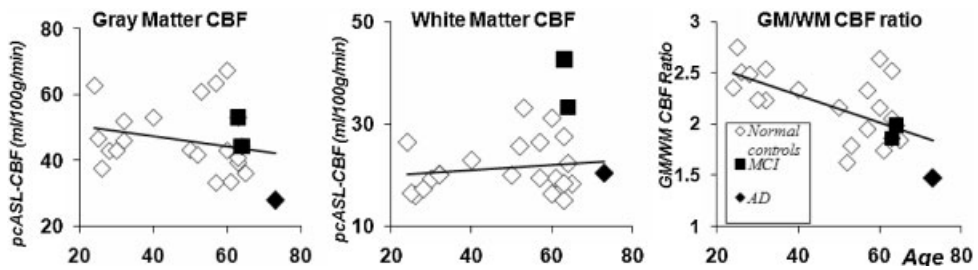

Figure 3. Global gray matter, white matter ROI CBF values and their ratios were plotted against age. No group difference was found in global gray matter and white matter perfusion values between the normal young and elderly subjects. The GM/WM ratio is significantly higher in young controls than the elderly subjects ($p < 0.009$, *t*-test). There are weak correlations between age and global GM perfusion (CC $= -0.24$, $p < 0.292$), WM perfusion (CC $= 0.17$, $p < 0.457$). Significant negative correlations was found between age and GM/WM perfusion ratio (CC $= -0.62$, $p < 0.002$).

NMR IN BIOMEDICINE

correlation (CC = −0.24) was found between age and GM CBF, there was no significant change of WM CBF with age increase. Interestingly, AD and MCI patients' GM/WM perfusion ratio values are among the lowest values of all the participants (Fig. 3).

DISCUSSION

Our results demonstrate that pcASL sequence could provide CBF measurement with high reliability in both young controls and older subjects. The normalized CBF images measured by pcASL were comparable to those obtained with ^{15}O-water PET scans on the same subjects including AD, MCI patients and elderly controls. A previous ASL study revealed that random noise contributed to the fluctuations in ASL perfusion signal more than the physiological variations within each subject (13). This finding indicated that the low SNR in ASL signal could potentially limit the measurement's reliability. Furthermore, a recent study showed that voxels in deep WM measured by ASL had a perfusion SNR less than one and ASL applicability became problematic (12). In order to improve perfusion SNR, the current pcASL technique in this study adapted a combination of several technical advances including a 3.0 Tesla scanner, a multi-channel receiver coil, pseudo-continuous ASL labeling, background static signal suppression and 3D segmented spiral acquisition.

First, the ASL perfusion signal is largely enhanced on 3.0 T compared to 1.5 T since both the blood T1 relaxation time and spin magnetization are increased with the magnetic field strength. Second, the pseudo-continuous tagging method achieves a high labeling efficacy with a standard coil setting by applying thousands of millisecond-long pulses to create the blood flow driven adiabatic inversion condition with minimized MT effect (17). Third, the static background signal is suppressed with null pulses to reduce the MT effect and improve the perfusion SNR (21). Fourth, a segmented multi-shot 3D spiral acquisition allows a very short TE and leads to less signal dropout and imaging distortion, especially in the frontal and temporal lobes where the susceptibility-induced problems are severe in typical echo planar images. With a combination of all the above technical improvements, the pcASL sequence used only ~5 min to collect the perfusion maps with a similar SNR to a recent ASL study with a 10 min long scan (12).

From the current ICC result, there is no difference in reliability of the ASL measurements between young and elderly subjects. However, the older subjects only had two pcASL scans while the young controls had three. The number of repeated measurements could directly affect the reliability outcome since ICC is a ratio outcome related to variance. When we randomly removed one pcASL scan result from the reliability analysis, the CBF reliability from the young subjects would increase and show slightly higher reliability than those ICC values from the older subjects. Increased reliability in young controls is consistent with the slightly higher perfusion SNR in young controls' CBF images in comparison to those in elderly subjects.

Cerebral blood flow is believed to be tightly coupled to brain neuronal activity and could be affected by various factors (33). A previous study with ^{15}O-water PET has reported 8% variation in white matter and 10% in gray matter for 2-day intervals (34). The current experiment was designed to study the instrumental error of pcASL CBF measurement, therefore the time frame of repeated measurements was within one hour. We expected that most of the variance in CBF value would arise from the measurement instead of physiological changes. In terms of ICC values, our pcASL reliability result is better than the previously reported CBF variation in both GM and WM with pulsed ASL technique (13). One important issue of perfusion measurement is the CBF variation across subjects. Roughly 20–25% percent variation across-subjects was observed forthe pcASL CBF mean values. Compared to young controls, elderly subjects showed greater variation overall. Besides the physiological CBF variation across subjects, one major concern about ASL signal is its labeling efficacy variation between subjects. Recent studies have shown high variation in pcASL inversion pulse labeling efficacy due to its sensitivity to the blood velocity (17,18). Before making conclusion of the high sensitivity of pcASL technique, a careful evaluation of ASL CBF signal with other absolute flow quantification methods is necessary.

Since we did not record the radioactivity of an arterial blood sample during the PET scan, the absolute value of CBF could not be quantified in the current ^{15}O-water PET experiment. However, the relative CBF (rCBF) values from PET scans showed a tight correlation to the quantitative ASL CBF values in the older subjects who received both scans. Using the Bland-Altman plot, the rCBF value difference between two methods was within the 95% CI range. This converging perfusion result in elderly subjects is consistent with the previous ASL-PET comparison in young controls (10). However, in the Bland-Altman plots of both GM and PCC ROIs, the agreement of two measurements remained lowest on the AD patient, whose perfusion was also lowest among all participants. This could suggest the perfusion variation depends strongly on the magnitude of measurement. Although the pcASL technique used a similar flow quantification mechanism as ^{15}O-water PET, the ASL model suffers from the fast decay of magnetization. Our current single compartment ASL model assumes that water of blood is instantaneously exchanged into tissue as soon as it reaches brain. Compared to the ^{15}O-water 2-minute half-life, the magnetically labeled water in ASL only has a 1-2 second half-life. The assumptions regarding exchange rate between blood/tissue compartments and the decay of the tag could bring error into the flow quantification and possibly over-estimate the derived CBF values. The heterogeneity of arterial transit time between subjects and different brain regions may further affect the precision of the flow quantification. Under the current 3.0 T field strength and 1.5 second post-labeling delay time, these above errors in the single compartment flow quantification model is likely to be limited to GM (11,16).

One interesting finding of the current study is that the GM to WM perfusion ratio decreases when the subject's age increases and such GM/WM ratios were especially lower among the MCI and AD patients. Although cerebral perfusion was previously reported to decrease with age at a rate of 0.45–0.7% per year, this pattern of age dependent CBF reduction may be nonlinear across stages of the lifespan (35–37). For example, by using ASL on 1.5 T MR system, a recent study found aging-related perfusion reductions in the frontal lobe (14) while another group reported a significant gap in CBF only between children and adult subjects, but much less CBF difference between adults and elderly subjects (38). Meanwhile, white matter perfusion rate changes remained stable against aging (39). In our current result, neither GM nor WM CBF is significantly different between the young and elderly controls. The correlations between age and GM or WM perfusion rates were not significant.

Several previous studies have reported hypo-perfusion in AD and MCI patients with ASL techniques (4,8,9,40) while other more recent studies found regional hyper-perfusion in the dementia

patients (41,42) that is indicative of brain compensation. Recent AD research has been focused on the elderly people who are at risk for developing AD. For example, it was reported that people at risk for AD exhibit compensatory increased perfusion in the mesial temporal lobes during resting ASL imaging (41,43). The test–retest of ASL technique has not been tested before with an at-risk cohort or AD patients. When there is a conflicting finding of increased and decreased perfusion during the early stage of AD, the reliability test becomes even more important. Our interpretation and hypothesis of the CBF change related to early AD brain adjustment for the loss of synapses and neurons certainly relies on the reliability and validity of the measurement itself. One encouraging finding from the current data is that the high ICC value of repeated pcASL CBF measures indicated good reliability among elderly subjects, including AD and MCI patients. An overall trend of slight CBF decrease with aging is found across all ROIs when comparing young and elderly subjects. However, none of these ROIs' CBF comparison yielded a statistically significant difference. A larger sample size and more sophisticated model such as multivariate analysis of different brain ROIs (40) would further help to depict the age-perfusion relationship. Interestingly, while MCI patients show similar perfusion rates compared to cognitively normal elderly subjects, their GM/WM ratios were close to values of the AD subjects and much lower than most controls. Due to the small patient number included in our current study, limited interpretation could be made to link this GM and WM perfusion change mismatch to early AD pathophysiological processes at this point.

Several limitations remain in this study. First, we did not sample the arterial blood radiation dosage during the ^{15}O-water PET scan. A quantitative CBF comparison from both ASL and PET methods would be more desirable to study the potential problems in the ASL quantification model. Fortunately, similar comparison work has been previously performed within the same group of adults and discrepancies between two CBF methods has been addressed (10,11). Second, we did not include arterial blood transit time or capillary permeability (exchange ratio between compartments) into the flow quantification. In order to measure the transit time, the protocol would require varying post-labeling delay, which would prohibitively increase the scan time. The precise measurement of the capillary permeability surface area product for the two-compartment flow model is also problematic under current MR capabilities (44). The overall effect of these factors on CBF values remains unclear and needs further investigation. Future longitudinal repeated CBF measurement would be very important to evaluate its usefulness in clinical environment.

CONCLUSION

The reliability of the quantitative perfusion imaging performed by 3D pseudo-continuous ASL has been studied on both young and elderly subjects on 3.0 T. Perfusion rates found between pcASL and ^{15}O-water PET perfusion scans had very good agreement in a subgroup of older subjects who were scanned by both imaging modalities. Compared to previous ASL and PET perfusion studies, the 3D pcASL technique offers as good or even better reliability in repeated CBF measurement among both young and elderly subjects. The relationship between quantitative ASL CBF, age and AD is consistent with previous reports, further validating the approach.

Acknowledgements

This research was supported by a Merit Review Grant from the Department of Veterans Affairs to SCJ. Additional support was provided by NIH AG21155, and AG20013, AG27161, and EB007021-03. This paper has a William S. Middleton Memorial VA Hospital GRECC manuscript of 2009–13.

REFERENCES

1. Huang C, Wahlund LO, Almkvist O, Elehu D, Svensson L, Jonsson T, Winblad B, Julin P. Voxel- and VOI-based analysis of SPECT CBF in relation to clinical and psychological heterogeneity of mild cognitive impairment. Neuroimage. 2003; 19(3): 1137–1144.
2. Harris GJ, Lewis RF, Satlin A, English CD, Scott TM, Yurgelun-Todd DA, Renshaw PF. Dynamic susceptibility contrast MR imaging of regional cerebral blood volume in Alzheimer disease: a promising alternative to nuclear medicine. AJNR. 1998; 19(9): 1727–1732.
3. Ishii K, Sasaki M, Yamaji S, Sakamoto S, Kitagaki H, Mori E. Demonstration of decreased posterior cingulate perfusion in mild Alzheimer's disease by means of H215O positron emission tomography. Eur. J. Nucl. Med. 1997; 24(6): 670–673.
4. Alsop DC, Detre JA, Grossman M. Assessment of cerebral blood flow in Alzheimer's disease by spin-labeled magnetic resonance imaging. Ann. Neurol. 2000; 47(1): 93–100.
5. Williams DS, Detre JA, Leigh JS, Koretsky AP. Magnetic resonance imaging of perfusion using spin inversion of arterial water. Proc. Natl. Acad. Sci. USA. 1992; 89(1): 212–216.
6. Buxton RB, Frank LR. A model for the coupling between cerebral blood flow and oxygen metabolism during neural stimulation. J. Cereb. Blood. Flow. Metab. 1997; 17(1): 64–72.
7. Floyd TF, Ratcliffe SJ, Wang J, Resch B, Detre JA. Precision of the CASL-perfusion MRI technique for the measurement of cerebral blood flow in whole brain and vascular territories. J. Magn. Reson. Imaging. 2003; 18(6): 649–655.
8. Xu G, Antuono PG, Jones J, Xu Y, Wu G, Ward D, Li SJ. Perfusion fMRI detects deficits in regional CBF during memory-encoding tasks in MCI subjects. Neurology. 2007; 69(17): 1650–1656.
9. Johnson NA, Jahng GH, Weiner MW, Miller BL, Chui HC, Jagust WJ, Gorno-Tempini ML, Schuff N. Pattern of cerebral hypoperfusion in Alzheimer disease and mild cognitive impairment measured with arterial spin-labeling MR imaging: initial experience. Radiology. 2005; 234(3): 851–859.
10. Ye FQ, Berman KF, Ellmore T, Esposito G, van Horn JD, Yang Y, Duyn J, Smith AM, Frank JA, Weinberger DR, McLaughlin AC. H(2)(15)O PET validation of steady-state arterial spin tagging cerebral blood flow measurements in humans. Magn. Reson. Med. 2000; 44(3): 450–456.
11. Donahue MJ, Lu H, Jones CK, Pekar JJ, van Zijl PC. An account of the discrepancy between MRI and PET cerebral blood flow measures. A high-field MRI investigation. NMR Biomed. 2006; 19(8): 1043–1054.
12. van Gelderen P, de Zwart JA, Duyn JH. Pittfalls of MRI measurement of white matter perfusion based on arterial spin labeling. Magn. Reson. Med. 2008; 59(4): 788–795.
13. Jahng GH, Song E, Zhu XP, Matson GB, Weiner MW, Schuff N. Human brain: reliability and reproducibility of pulsed arterial spin-labeling perfusion MR imaging. Radiology. 2005; 234(3): 909–916.
14. Parkes LM, Rashid W, Chard DT, Tofts PS. Normal cerebral perfusion measurements using arterial spin labeling: reproducibility, stability, and age and gender effects. Magn. Reson. Med. 2004; 51(4): 736–743.
15. Yen YF, Field AS, Martin EM, Ari N, Burdette JH, Moody DM, Takahashi AM. Test-retest reproducibility of quantitative CBF measurements using FAIR perfusion MRI and acetazolamide challenge. Magn. Reson. Med. 2002; 47(5): 921–928.
16. Campbell AM, Beaulieu C. Pulsed arterial spin labeling parameter optimization for an elderly population. J. Magn. Reson. Imaging. 2006; 23(3): 398–403.
17. Dai W, Garcia D, de Bazelaire C, Alsop DC. Continuous flow-driven inversion for arterial spin labeling using pulsed radio frequency and gradient fields. Magn. Reson. Med. 2008; 60(6): 1488–1497.
18. Wu WC, Fernandez-Seara M, Detre JA, Wehrli FW, Wang J. A theoretical and experimental investigation of the tagging efficiency of

pseudocontinuous arterial spin labeling. Magn. Reson. Med. 2007; 58(5): 1020–1027.
19. Wang J, Alsop DC, Li L, Listerud J, Gonzalez-At JB, Schnall MD, Detre JA. Comparison of quantitative perfusion imaging using arterial spin labeling at 1.5 and 4.0 Tesla. Magn. Reson. Med. 2002; 48(2): 242–254.
20. Sager MA, Hermann B, La Rue A. Middle-aged children of persons with Alzheimer's disease: APOE genotypes and cognitive function in the Wisconsin Registry for Alzheimer's Prevention. J. Geriatr. Psychiatry Neurol. 2005; 18(4): 245–249.
21. Ye FQ, Frank JA, Weinberger DR, McLaughlin AC. Noise Reduction in 3D Perfusion Imaging by Attenuating the Static Signal in Arterial Spin Tagging (ASSIST). Magn. Reson. Med. 2000; 44(1): 92–100.
22. Williams DS, Detre JA, Leigh JS, Koretsky AP. Magnetic Resonance Imaging of Perfusion Using Spin Inversion of Arterial Water. Proc. Natl. Acad. Sci USA. 1992; 89: 212–216.
23. Alsop DC, Detre JA. Reduced transit-time sensitivity in non-invasive Magnetic Resonance Imaging of human cerebral blood flow. J. Cereb. Blood. Flow. Metab. 1996; 16: 1236–1249.
24. Buxton RB, Frank LR, Wong EC, Siewert B, Warach S, Edelman RR. A general kinetic model for quantitative perfusion imaging with arterial spin labeling. Magn. Reson. Med. 1998; 40(3): 383–396.
25. Herscovitch P, Raichle ME. What is the correct value for the brain––blood partition coefficient for water? J. Cereb. Blood. Flow. Metab. 1985; 5(1): 65–69.
26. Alsop DC, Detre JA. Multisection cerebral blood flow MR imaging with continuous arterial spin labeling. Radiology. 1998; 208(2): 410–416.
27. Maccotta L, Detre JA, Alsop DC. The efficiency of adiabatic inversion for perfusion imaging by arterial spin labeling. NMR. Biomed. 1997; 10(4–5): 216–221.
28. Alsop D. *Improved Efficiency for Multi-Slice Continuous Arterial Spin Labeling Using Time Varying Gradients*. International Society for Magnetic Resonance in Medicine: Glasgow, 2001; pp. 1562.
29. Garcia DM, Duhamel G, Alsop DC. Efficiency of inversion pulses for background suppressed arterial spin labeling. Magn. Reson. Med. 2005; 54(2): 366–3372.
30. Carson R, Daube-Witherspoon M, Herscovitch P. *Quantitative Functional Brain Imaging With Positron Emission Tomography*. Academic Press: London, 1998.
31. Shrout PE, Fleiss JL. Intraclass correlations: uses in assessing rater reliability. Psychologic. Bull. 1979; 86(2): 420–428.
32. Altman DG, Bland JM. Measurement in medicine: the analysis of method comparison studies. Statistician. 1983; 32(3): 307–317.
33. Lassen NA. Cerebral blood flow and oxygen consumption in man. Physiol. Rev. 1959; 39(2): 183–238.
34. Carroll TJ, Teneggi V, Jobin M, Squassante L, Treyer V, Hany TF, Burger C, Wang L, Bye A, Von Schulthess GK, Buck A. Absolute quantification of cerebral blood flow with magnetic resonance, reproducibility of the method, and comparison with H2(15)O positron emission tomography. J. Cereb. Blood. Flow. Metab. 2002; 22(9): 1149–1156.
35. Pantano P, Baron JC, Lebrun-Grandie P, Duquesnoy N, Bousser MG, Comar D. Effects of normal aging on regional CBF and CMRO2 in humans. Monogr. Neural. Sci. 1984; 11: 123–130.
36. Leenders KL, Perani D, Lammertsma AA, Heather JD, Buckingham P, Healy MJ, Gibbs JM, Wise RJ, Hatazawa J, Herold S, *et al*. Cerebral blood flow, blood volume and oxygen utilization. Normal values and effect of age. Brain. 1990; 113(Pt 1): 27–47.
37. Martin AJ, Friston KJ, Colebatch JG, Frackowiak RS. Decreases in regional cerebral blood flow with normal aging. J. Cereb. Blood. Flow. Metab. 1991; 11(4): 684–689.
38. Biagi L, Abbruzzese A, Bianchi MC, Alsop DC, Del Guerra A, Tosetti M. Age dependence of cerebral perfusion assessed by magnetic resonance continuous arterial spin labeling. J. Magn. Reson. Imaging. 2007; 25(4): 696–702.
39. Shin W, Horowitz S, Ragin A, Chen Y, Walker M, Carroll TJ. Quantitative cerebral perfusion using dynamic susceptibility contrast MRI: evaluation of reproducibility and age- and gender-dependence with fully automatic image postprocessing algorithm. Magn. Reson. Med. 2007; 58(6): 1232–1241.
40. Asllani I, Habeck C, Scarmeas N, Borogovac A, Brown TR, Stern Y. Multivariate and univariate analysis of continuous arterial spin labeling perfusion MRI in Alzheimer's disease. J. Cereb. Blood. Flow. Metab. 2008; 28(4): 725–736.
41. Alsop DC, Casement M, de Bazelaire C, Fong T, Press DZ. Hippocampal hyperperfusion in Alzheimer's disease. Neuroimage. 2008; 42(4): 1267–1274.
42. Dai W, Lopez OL, Carmichael OT, Becker JT, Kuller LH, Gach HM. Mild cognitive impairment and alzheimer disease: patterns of altered cerebral blood flow at MR imaging. Radiology. 2009; 250(3): 856–866.
43. Fleisher AS, Podraza KM, Bangen KJ, Taylor C, Sherzai A, Sidhar K, Liu TT, Dale AM, Buxton RB. Cerebral perfusion and oxygenation differences in Alzheimer's disease risk. Neurobiol. Aging. 2008.
44. Carr JP, Buckley DL, Tessier J, Parker GJ. What levels of precision are achievable for quantification of perfusion and capillary permeability surface area product using ASL? Magn. Reson. Med. 2007; 58(2): 281–289.